A multi-feature fusion-based change detection method for remote sensing images

Liping Cai[1,2*], Wenzhong Shi[3*], Ming Hao[4], Hua Zhang[4], and Lipeng Gao[5]

Abstract

An object-oriented change detection method for remote sensing images based on multiple features using a novel weighted fuzzy c-means (WFCM) method is presented. First, Gabor and Markov random field textures are extracted and added to the original images. Second, objects are obtained by using a watershed segmentation algorithm to segment the images. Third, simple threshold technology is applied to produce the initial change detection results. Finally, refining is conducted using WFCM with different feature weights identified by the Relief algorithm. Two satellite images are used to validate the proposed method. Experimental results show that the proposed method can reduce uncertainties involved in using a single feature or using equally-weighted features, resulting in higher accuracy.

Keywords multi-feature fusion, feature weight, fuzzy C-means, object-oriented change detection

1. Introduction

Change detection from multi-temporal remote sensing images can quickly yield information on terrestrial modifications, such as land-cover changes, urban expansion, vegetation changes, and climate change (Jin et al. 2013). Hence, change detection is widely used for such tasks as updating geographic data, monitoring land use, monitoring ecology, and predicting and assessing disaster (Lu et al. 2004). With the advent of modern remote sensing technology, spatial resolution of remote sensing images has been constantly improving. As a result, more attention has been paid to object-oriented change detection methods than traditional methods (Aguirre-Gutiérrez et al. 2012).

Traditional algebraic methods obtain changes by comparing spectral features of multi-temporal images (Kennedy et al. 2009). As the resolution of a remote sensing image increases, textural features, geometrical features, and spatial relations, in

* Liping Cai, cumtcailp@126.com
Wenzhong Shi, lswzshi@polyu.edu.hk

[1] School of Geography and Tourism, Qufu Normal University, Rizhao, China; [2] Key Laboratory of Coastal Zone Exploitation and Protection, Ministry of Land and Resource, Nanjing, China; [3] Department of Land Surveying and Geo-Informatics, The Hong Kong Polytechnic University, Hong Kong, China; [4] School of Environment Science and Spatial Informatics, China University of Mining and Technology, Xuzhou, China; [5] School of Remote Sensing and Information Engineering, Wuhan University, Wuhan, China.

addition to spectral features, can be combined for change detection (Liu et al. 2012). Rather than using a single feature, multiple features can provide complementary information that is independent and, thus, improves the reliability of change detection. The reason is that using multiple features can integrate the advantages while compress the limitations of using different features (Ma et al. 2012). The Gabor (Riaz et al. 2013) and Markov random field (MRF) textures (Wang and Bai 2006) are typical image textures. They have already been applied successfully to image processing (Clausi 2001). Besides the algebraic method, fuzzy c-means (FCM) (Bezdek et al. 1984), a clustering method, has also been successfully used in change detection. FCM can exploit multiple features for change detection. In general, different features will produce different change detection accuracies (Du et al. 2012), so it is rational to consider feature weighting, rather than using a uniform feature weight, to improve the change detection performance. In the last few years, a large number of change detection methods have appeared (Hussain et al. 2013; Lv et al. 2018a). In particular, due to increases in spatial resolution, object-oriented change detection methods have attracted much attention (Silveira et al. 2018， Lv et al. 2018b).

Based on the aforementioned analysis, an object-oriented change detection method relying on multiple features and weighted fuzzy c-means (WFCM) was used in this study. In this method, Gabor and MRF textures of images are first extracted. Next, to obtain the basic unit of object-oriented change detection, a watershed segmentation algorithm (Cai et al. 2015) is adopted to segment the stacked image from two temporal images. In this step, the mean feature value of all pixels in the object is set as the feature value of the object for all features. Afterwards, the weights of different features are calculated by using the Relief algorithm, based on the initial change detection result obtained by the histogram threshold method (Otsu 1979). Finally, WFCM is used to combine multiple features (spectral feature, Gabor texture, and MRF texture) and obtain the change detection results.

2. Methods

Let $\mathbf{X}_1$ and $\mathbf{X}_2$ be two multispectral images with B bands, acquired in the same geographical area at two different times. Such images are assumed to have been preprocessed well, including the application of radiometric calibration and co-registration. The Gabor (Riaz et al. 2013) and MRF textures (Wang and Bai 2006) are extracted from the multispectral images at different times. The feature differences $\mathbf{D} = \mathbf{X}_1 - \mathbf{X}_2$ are generated by subtracting the feature values for each pixel of the two images. The multi-temporal images are superimposed before segmenting the images. The superimposed images are segmented by a watershed segmentation algorithm and the spectral feature, texture feature, and spatial relation are fused to control the object scale in order to obtain a satisfactory segmentation scale. Further details of the watershed segmentation algorithm are given by Cai et al. (2015). Fig. 1 displays the flowchart summarizing the proposed method.

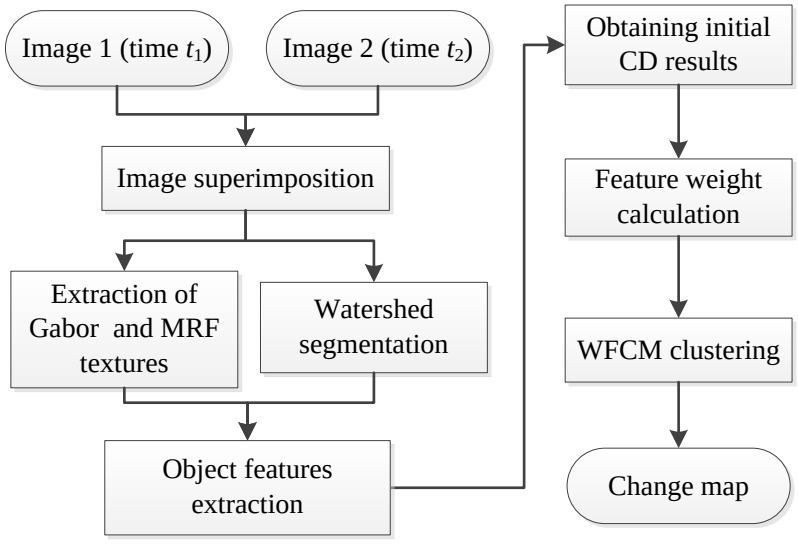

Fig. 1 Flowchart of the proposed method

2.1 Feature weight calculation

Spectral features, textural features, spatial relations, and other features can be applied for object-oriented change detection. In this study, the spectral feature, Gabor texture, and MRF texture are chosen as the features for change detection. Considering that different features have different effects on change detection results, the results are obtained by different features with different accuracies. The Relief algorithm (Sun 2007) is considered to be one of the most successful for image processing due to its simplicity and effectiveness. This algorithm calculates the feature weight according to the feature distance of samples. If the sample feature distance from the same class is smaller and the sample feature distance from different classes is larger, then the feature weight will be larger. The Relief algorithm is used to calculate the feature weight at the map level. The principle of the Relief algorithm is as follows:

$$w_{d,t} = w_{d,t-1} + \frac{P_{d,\mathrm{H}}(t)}{l} - \frac{P_{d,\mathrm{S}}(t)}{l}, \tag{1}$$

where $w_{d,t}$ is the weight of feature *d* at the *t*th iteration, the iteration ends at the *l*th time, *l* is the number of samples, and the initialization of $w_{d,0}$ is set to zero. $P_{d,\mathrm{S}}(t)$ and $P_{d,\mathrm{H}}(t)$ represent the feature distances between the *t*th sample from its closest similar sample and from its closest heterogeneous sample in terms of feature *d*, respectively. The samples comprise two classes (changed and unchanged). The initial change detection results are obtained by the histogram threshold method (Otsu 1979) to classify the objects into two classes. Many objects have the same feature value, and, thus, to increase computational efficiency, the samples are selected by random sampling from the initial change detection results.

2.2 Weighted fuzzy c-means clustering

FCM clustering is an improved c-means clustering method (Bezdek et al. 1984). For most practical applications, using the FCM clustering method weights each feature equally, which may decrease change detection performance in this application. After the weight of the object feature in change detection is calculated, the objective function of FCM is improved according to the weight of the feature. The objective function contains a measured distance $\|\bullet\|$, the Euclidean distance. In this study, the weighted Euclidean distance is adopted as the measured distance, as follows,

$$\left\|\boldsymbol{x}_i-\boldsymbol{v}_j\right\|=\sqrt{\sum_{d=1}^{D} w_d\left(x_{id}-v_{jd}\right)^2}, \tag{2}$$

where $\boldsymbol{x}_i$ represents the feature values of the *i*th object in the difference image, x_{id} is the *d*th feature value of *i*th object in the difference image, $\boldsymbol{v}_j$ is the *j*th cluster centre, v_{jd} is the *d*th feature value of *j*th cluster centre, w_d is the weight of the *d*th feature, which is calculated by Equation (1), and *D* is the number of features. Therefore, the improved objective function J of FCM is defined as

$$J=\sum_{j=1}^{Y}\sum_{i=1}^{N} u_{ij}^{r}\sum_{d=1}^{D} w_d\left(x_{id}-v_{jd}\right)^2, \tag{3}$$

where u_{ij} is the membership probability of *i*th object belonging to *j*th cluster, *Y* is the number of clusters, *N* is the number of objects, and $r\in[1,\infty)$ is the weighted index, set to two in this study. Membership probability u_{ij} is computed as follows,

$$u_{ij}=\frac{\sum_{d=1}^{D} w_d\left(x_{id}-v_{jd}\right)^{-2}}{\sum_{t=1}^{Y}\sum_{d=1}^{D} w_d\left(x_{id}-v_{jd}\right)^{-2}}. \tag{4}$$

The cluster centre $\boldsymbol{v}_j$ is defined as

$$\boldsymbol{v}_j=\frac{\sum_{i=1}^{N} u_{ij}^{l}\boldsymbol{x}_i}{\sum_{i=1}^{N} u_{ij}^{l}}. \tag{5}$$

Further details about FCM can be found in Bezdek et al. (1984). WFCM is adopted, which divides objects into two classes (i.e., changed and unchanged) by fusing multiple features.

3. Experiments

In this section, two satellite images from Landsat TM and SPOT-5 were used to evaluate the proposed method. In this study, missed detections, false alarms, and total error (He et al. 2014) are used to quantitatively evaluate the proposed method. The Gabor textures were extracted from the images using width, scale, and direction parameters of 5, 5, and 12, respectively. A 3-pixel × 3-pixel window and second-order Gauss MRF model were used to extract MRF textures from images. The experiments were conducted on a PC with an Intel Core2Quad processor at a clock speed of 1.80 GHz. MATLAB® was used to program the proposed method.

3.1 Experiment 1

Data used in Experiment 1 were Landsat TM satellite images with a spatial resolution of 30 m per pixel and an area of 2000 pixels × 2000 pixels, which were acquired in July 2000 (t_1) and July 2006 (t_2) in Rondonia, Brazil (see Fig. 2). The study area is located in the Amazon forest area, which is usually covered with forest and farmland. From 2000 to 2006, a large area shifted from forest to farmland due to agricultural development, causing significant vegetation reduction in this area. Fig. 3(a) shows a ground reference map of the changes that were manually obtained.

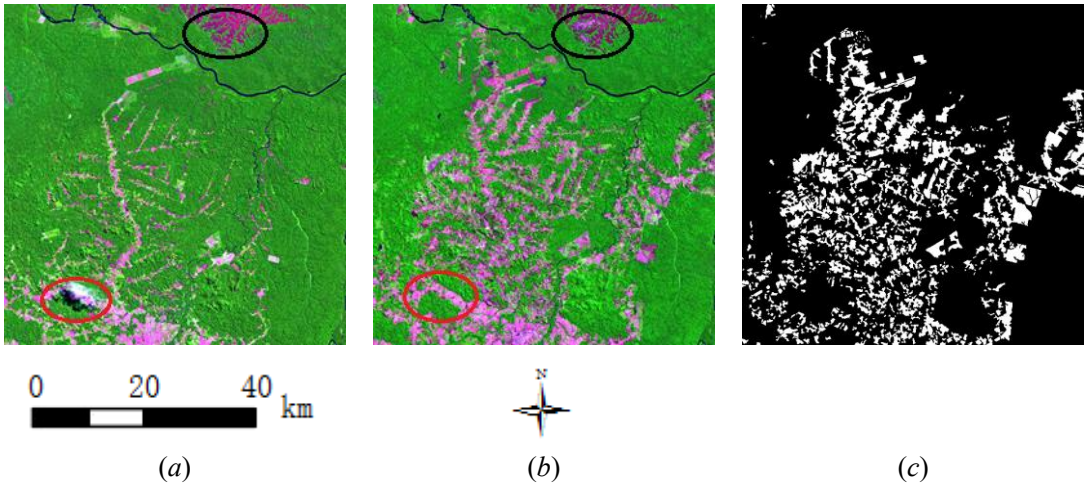

Fig. 2 Landsat TM remote sensing images with six multispectral bands (bands 5, 4, and 3 were used for display; the centre coordinate: 09° 09′ 48.14″ S, 61° 57′ 53.39″ W) acquired in (*a*) July 2000 and (*b*) July 2006, (*c*) reference data

Fig. 3(*b*)–3(*h*) presents change detection results of the proposed method using different feature sets. Fig. 2 shows that, considering the influence of clouds, in the red ellipse region of the t_1 image, the spectral information is abnormal. In the black ellipse region, although the ground covering categories in the two temporal images are similar, significant differences are observed in terms of spectral feature, because of the effect of imaging conditions. Through the comparisons between the reference data and Fig. 3(*b*)–3(*d*), change detection results obtained by using the spectral feature have the most obvious false detections, and the change detection results obtained by using the Gabor

texture have the fewest false detections in the two corresponding ellipse areas. Due to the comparisons between the reference data and Fig. 3(*e*)–3(*g*), change detection results obtained by fusing the spectral feature and MRF texture have relatively the highest false detection, and change detection results obtained by fusing Gabor texture and MRF texture have relatively the lowest false detection in the two corresponding ellipse areas. Table 1 reports the quantitative results of experiment 1. In the change detection results obtained on the basis of a single feature, the change detection results obtained by using the MRF texture have the largest number of false alarms and the highest total error. The change detection results obtained by using the spectral feature have the largest number of missed detection events. The change detection results obtained by using Gabor texture have the smallest number of false alarms, lowest number of missed detections, and lowest total error. When fusing two features, only the missed detections from the change detection results obtained by fusing the spectral feature and MRF texture increased. The missed detections, false alarms, and total error of the other change detection results decreased at the same time. Finally, after fusing three features, the missed detections, false alarms, and total error of the change detection results also decreased. Considering both visual and quantitative assessments, feature fusion achieves a complement of features and reduces the total error in the change detection results, thus, improving the accuracy of the change detection results.

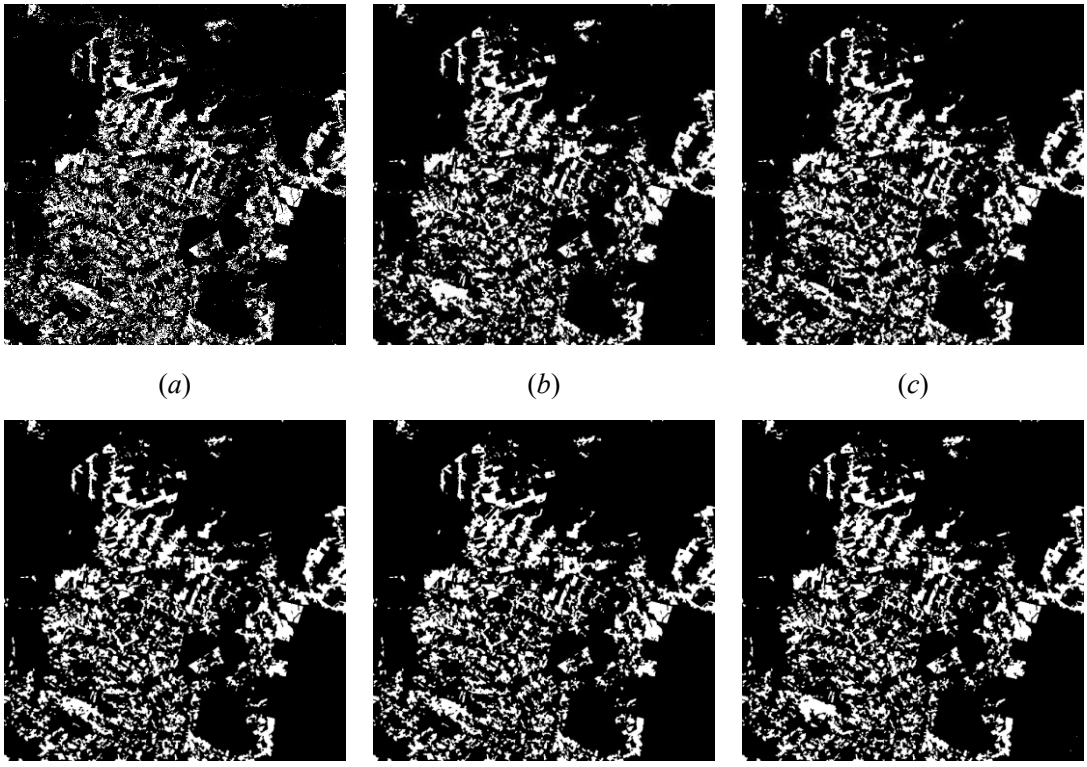

(*a*) (*b*) (*c*)

(*d*) (*e*) (*f*)

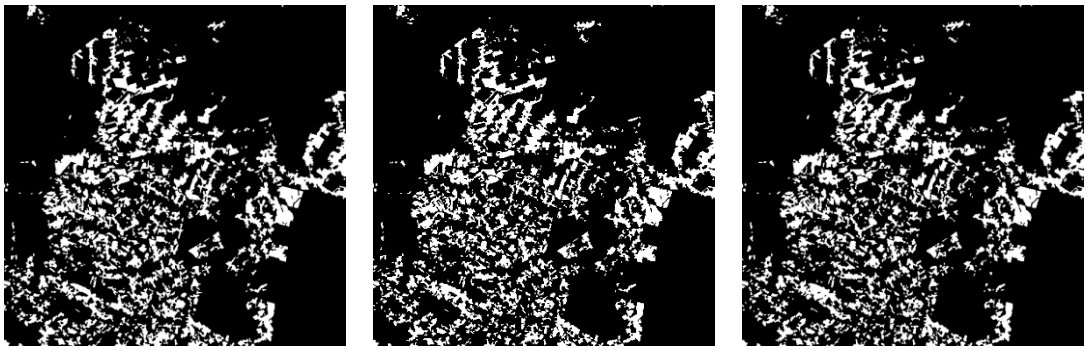

(*g*) (*h*) (*i*)

Fig. 3 Change detection results obtained by using different features from Landsat TM remote sensing images. (*a*) Pixel, (*b*) spectral feature, (*c*) Gabor texture, (*d*) MRF texture, (*e*) fusion of spectral feature and Gabor texture, (*f*) fusion of spectral feature and MRF texture, (*g*) fusion of Gabor texture and MRF texture, (*h*) equal fusion of three features, and (*i*) weighted fusion of three features

Table 1. Accuracy of experiment results

Features	Missed detections		False alarms		Total errors	
	No. of pixels	%	No. of pixels	%	No. of pixels	%
Pixel	155075	23.62	147129	4.40	302204	7.56
Spectrum	71790	10.94	100749	3.01	172539	4.31
Gabor	62703	9.55	99210	2.97	161913	4.05
MRF	64043	9.76	145554	4.35	209597	5.24
Spectrum+Gabor	59666	9.09	77291	2.31	136957	3.42
Spectrum+MRF	73290	11.16	97445	2.91	170735	4.27
Gabor+MRF	56052	8.54	105550	3.16	161602	4.04
Equal fusion of three features	56894	8.67	83263	2.49	140157	3.50
Weighted fusion of three features	54126	8.24	76759	2.30	130885	3.27

3.2 Experiment 2

The data used in Experiment 2 are pan-sharpened SPOT-5 satellite images with a spatial resolution of 2.5 m per pixel and an area of 2001 pixels × 1601 pixels, which were acquired in April 2008 (t_1) and February 2009 (t_2) in Tianjin, China (Fig. 4). The study area is covered with vegetation, building, roads, water, and bare land. Given that the study area is located in the urban outskirts, significant changes are observed in a short period of time. The changes mainly include building construction and demolition, and the ground reference map of changes was manually obtained and displayed in Fig. 5(*a*).

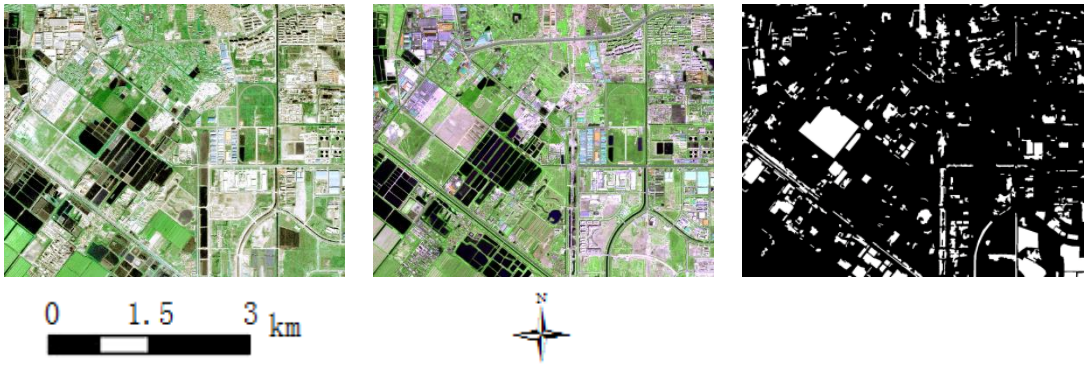

(*a*) (*b*) (*c*)

Fig. 4 SPOT 5 remote sensing images fused with panchromatic and multispectral bands (the centre coordinate: 39° 06′ 25.75″ N, 117° 03′ 10.68″ E) acquired in (*a*) April 2008 and (*b*) February 2009. (*c*) Reference data

Fig. 5(*b*)–5(*h*) present change detection results of the proposed method using different feature sets. In the change detection results obtained by a single feature, the missed detections, false alarms, and total error of the change detection results obtained by using the MRF texture are the highest; by contrast, the total error of the change detection results obtained by using Gabor texture is the lowest (Table 2). When fusing two features, both the missed detections and false alarms are reduced or, at least, one parameter is reduced. Moreover, the total error is reduced in all cases. When fusing three features, the missed detections of the change detection results are larger than those from the change detection results fusing the spectral feature and Gabor feature. However, the false alarms and total error are the lowest for all the change detection results. These findings show that the change detection results from fusing multiple features can reduce missed detections and false alarms, thereby improving the accuracy of the change detection results. This result also indicates that fusing multiple features can integrate the advantages and mitigate the limitations of different features. Therefore, the change detection results obtained by fusing multiple features are more accurate than the results obtained by using a single feature.

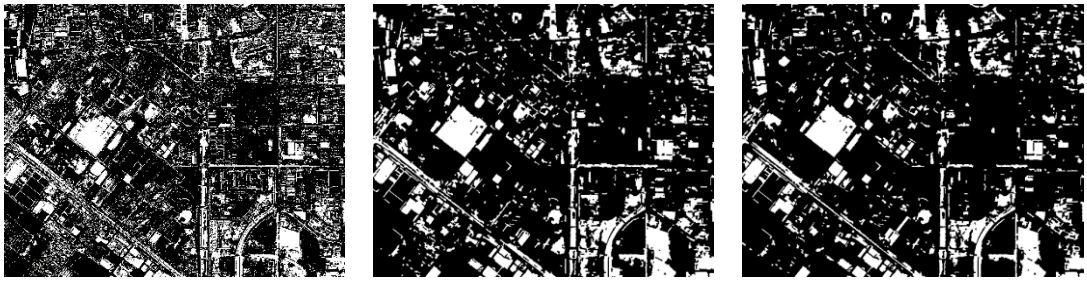

(*a*) (*b*) (*c*)

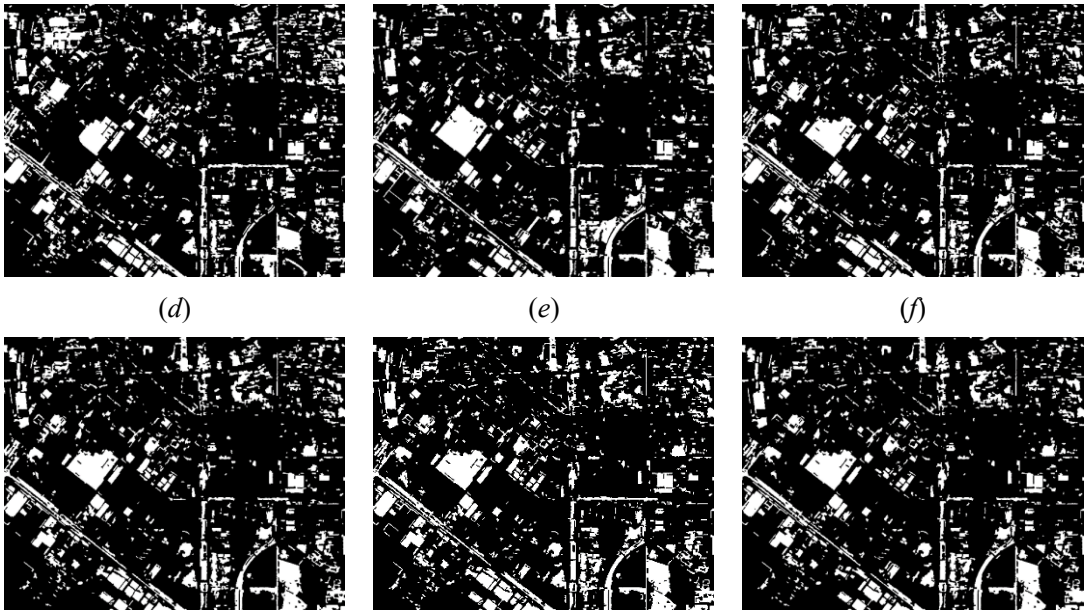

(*d*) (*e*) (*f*)

(*g*) (*h*) (*i*)

Fig. 5 Change detection results obtained by using different features from SPOT 5 remote sensing images. (*a*) Pixel, (*b*) spectral feature, (*c*) Gabor texture, (*d*) MRF texture, (*e*) fusion of spectral feature and Gabor texture, (*f*) fusion of spectral feature and MRF texture, (*g*) fusion of Gabor texture and MRF texture, (*h*) equal fusion of three features, and (*i*) weighted fusion of three features

Table 2. Accuracy of experiment results

Features	Missed detections		False alarms		Total errors	
	No. of pixels	%	No. of pixels	%	No. of pixels	%
Pixel	83515	18.49	464002	16.86	547517	17.09
Spectrum	26513	5.87	231780	8.42	258293	8.06
Gabor	41945	9.28	176332	6.41	218277	6.81
MRF	109444	24.23	267867	9.73	377311	11.78
Spectrum+Gabor	34872	7.72	169166	6.15	204038	6.37
Spectrum+MRF	44609	9.87	176310	6.41	220919	6.90
Gabor+MRF	44644	9.88	164352	5.97	208996	6.52
Equal fusion of three features	39493	8.74	176113	6.40	215606	6.73
Weighted fusion of three features	39705	8.79	140146	5.09	179851	5.61

3.3 Discussion

From the experiments, it can be seen that multi-feature fusion can improve the accuracy of object-oriented change detection. For the two experiments, the accuracies of the three-feature fusion change detection results were 1.26% and 3.27% higher than those for the single-feature fusion change detection results on average, and 0.64% and 0.99% higher than those for the two-feature fusion change detection results on average,

respectively. Fusing the various difference images integrated the advantages of different features to overcome the limitations of using different features for object-oriented change detection. The accuracies of the weighted fusion change detection results were 0.23% and 1.12% higher than that of the equal-weight fusion change detection results, respectively. The Relief algorithm considers prior knowledge, which is one reason why the results obtained from the fused difference image based on the Relief algorithm had the higher accuracy. The experimental analysis indicated that the weighted fusing of several difference images based on the Relief algorithm improved the accuracy of the change detection results.

4. Conclusion

In this study, we proposed a novel object-oriented change detection method for remote sensing images. Considering that different features produce different uncertainties in the change detection results of remote sensing images, the primary goal of this research is to improve the reliability of change detection results by fusing multiple features. The proposed method fuses multiple features to detect changes on the basis of an improved FCM, according to the separability of different features. The experimental results show that the proposed method can effectively improve the accuracy of change detection results. Limitations and uncertainties caused by a single feature can be reduced by fusing multiple features.

Further research will focus on the extraction of object features to better enhance the accuracy of the object-oriented change detection results. Moreover, decision-level fusion techniques will be considered to improve the final results.

Acknowledgments

This work was supported partly by the National Natural Science Foundation of China (41331175), A Project of Shandong Province Higher Educational Science and Technology Program (J17KA064), and the Open Fund of Key Laboratory of Coastal Zone Exploitation and Protection, Ministry of Land and Resource (2017CZEPK02).

References

Aguirre-Gutiérrez J, A. C. Seijmonsbergen, J. F. Duivenvoorden. 2012. Optimizing land cover classification accuracy for change detection, a combined pixel-based and object-based approach in a mountainous area in Mexico. *Applied Geography* 34: 29–37.

Bezdek, J.C., R. Ehrlich, and W. Full. 1984. FCM: the fuzzy c-means clustering algorithm. *Computers & Geosciences* 10(2-3), 191–203.

Cai, L., W. Shi, P. He, Z. Miao, M. Hao, and H. Zhang. 2015. Fusion of multiple features to produce a segmentation algorithm for remote sensing images. *Remote Sensing Letters* 6(5): 390–398.

Clausi, D. A. 2001. Comparison and fusion of co-occurrence, Gabor and MRF texture features for classification of SAR sea-ice imagery. *Atmosphere-Ocean* 39(3), 183–194.

Du, P., S. Liu, P. Gamba, K. Tan, and J. Xia. 2012. Fusion of Difference Images for Change Detection Over Urban Areas. *IEEE Journal of Selected Topics in Applied Earth Observations and Remote Sensing* 5(4): 1076–1086.

He P., W. Shi, Z. Miao, H. Zhang, and M. Hao. 2014. A novel dynamic threshold method for unsupervised change detection from remotely sensed images. *Remote Sensing Letters* 5(4): 396-403.

Hussain, M., D. Chen, A. Cheng, H. Wei, and D. Stanley. 2013. Change detection from remotely sensed images: from pixel-based to object-based approaches. *Isprs Journal of Photogrammetry & Remote Sensing* 80(2): 91–106.

Jin, S., L.Yang, P. Danielson, C. Homer, J. Fry, and G. Xian. 2013. A comprehensive change detection method for updating the national land cover database to circa 2011. *Remote Sensing of Environment* 132(10): 159–175.

Kennedy, R. E., P. A. Townsend, J. E Gross, W. B. Cohen, P. Bolstad, Y. Q. Wang, P. Bolstad, Y.Q. Wang, and P. Adams. 2009. Remote sensing change detection tools for natural resource managers: understanding concepts and tradeoffs in the design of landscape monitoring projects. *Remote Sensing of Environment* 113(7), 1382–1396.

Liu, X., Y. Shang, Z. Lei, and Q. Yu. 2012. Change detection by local illumination compensation using local binary pattern. *Optical Engineering* 51(9), 1487–1489.

Lu, D., P. Mausel, E. Brondízio, and E. Moran. 2004. Change detection techniques. *International Journal of Remote Sensing* 25(12): 2365–2401.

Lv, Z., T. Liu, P. Zhang, J. Benediktsson, and Y. chen. 2018. Land Cover Change Detection Based on Adaptive Contextual Information Using Bi-Temporal Remote Sensing Images. *Remote Sensing* 10(6): 901.

Lv, Z., T. Liu, Y. Wan, J. Benediktsson, and X. Zhang. 2018. Post-Processing Approach for Refining Raw Land Cover Change Detection of Very High-Resolution Remote Sensing Images. *Remote Sensing* 10(3): 472.

Ma, J., M. Gong, and Z. Zhou. 2012. Wavelet Fusion on Ratio Images for Change Detection in SAR Images. *IEEE Geoscience and Remote Sensing Letters* 9(6): 1122–1126.

Silveira, E., J. Mello, F. Júnior, and L. Carvalho. 2018.Object-based land-cover change detection applied to Brazilian seasonal savannahs using geostatistical features. *International Journal of Remote Sensing* 39(8): 2597-2619.

Sun, Y. 2007. Iterative relief for feature weighting: algorithms, theories, and applications. *IEEE Transactions on Pattern Analysis & Machine Intelligence* 29(6): 1035-1051.

Otsu, N. 1979. A threshold selection method from gray-level histogram. *IEEE Transaction on System Man and Cybernetics* 9(2): 62–65.

Riaz, F., A. Hassan, S. Rehman, and U. Qamar. 2013. Texture classification using rotation- and scale-invariant gabor texture features. *IEEE Signal Processing Letters* 20(6): 607–610.

Wang, K., X. Bai. 2006. Classification of wood surface texture based on Gauss-MRF Model. *Journal of Forestry Research* 17(1):57-61.

Vincent, L., and P. Soille. 1991. Watersheds in digital spaces: an efficient algorithm based on immersion simulations. *IEEE Transactions on Pattern Analysis and Machine Intelligence* 13(6): 583-598.